NGC 2548: clumpy spatial and kinematic structure in an intermediate-age Galactic cluster

Belén Vicente,[1] Néstor Sánchez[1,2]★ and Emilio J. Alfaro[1]

[1]*Instituto de Astrofísica de Andalucía, CSIC, Glorieta de la Astronomía s/n, E-18008 Granada, Spain*
[2]*Departamento de Física, Universidad de Murcia, E-30100 Murcia, Spain*

ABSTRACT

NGC 2548 is a ∼400–500 Myr old open cluster with evidence of spatial substructures likely caused by its interaction with the Galactic disc. In this work we use precise astrometric data from the *Carte du Ciel* – San Fernando (CdC-SF) catalogue to study the clumpy structure in this cluster. We confirm the fragmented structure of NGC 2548 but, additionally, the relatively high precision of our kinematic data lead us to the first detection of substructures in the proper motion space of a stellar cluster. There are three spatially separated cores each of which has its own counterpart in the proper motion distribution. The two main cores lie nearly parallel to the Galactic plane whereas the third one is significantly fainter than the others and it moves towards the Galactic plane separating from the rest of the cluster. We derive core positions and proper motions, as well as the stars belonging to each core.

Key words: stars: kinematics and dynamics – open clusters and associations: general – open clusters and associations: individual: NGC 2548.

1 INTRODUCTION

It is generally accepted that most stars (between 70 and 90 per cent) are born in star clusters (Lada & Lada 2003; Piskunov et al. 2008), which are naturally associated with high-density regions in molecular clouds (Elmegreen & Efremov 1996; Elmegreen 2006). Few million years after its formation, the number of observed clusters falls drastically (Oort 1958; Wielen 1971; Lada 2010). A rapid disruption of these stellar systems, which affects a high proportion of them, occurs at early dynamical evolutionary stages when embedded clusters remove their gas component (Tutukov 1978). At this time, stellar winds from massive stars and ejected matter from supernova explosions dissipate parental intra-cluster gas. If kinetic energy of the stars exceeds the remaining gravitational potential then the cluster quickly dilutes the primordial assembly into the stellar Galactic field. Only ∼10 per cent of the number of original clusters seem to survive the so-called 'infant mortality' and remain bound for longer than 1 Gyr (Fall, Chandar & Whitmore 2005). Surviving stellar clusters are suffering processes of partial destruction and dissipation during their whole life, whose true nature and details are still matter of debate although several global scenarios have been proposed in the last years (e.g. Elmegreen & Hunter 2010). Tidal Galactic field and encounters with giant molecular clouds are two main mechanisms responsible for the dissipation and disruption of stellar clusters, but the total lifetime of these systems and the rate at which they are loosing stars are very dependent on clus-

ter initial conditions (Elmegreen & Hunter 2010) and on the main destruction mechanism; for example, it has been shown that a star cluster can be disrupted even by a single tidal encounter with a giant molecular cloud (Kruijssen et al. 2011). Thus, initial mass, spatial distribution of zero-age stars, Galactic location and local environment of the birth place affect the dynamical evolution of stellar clusters for the first several hundred million years (Parker 2014; Parker et al. 2014).

Observations indicate that most embedded clusters, as well as some intermediate-age systems which have already lost their parental gas component, may exhibit a clumpy structure formed by several connected blobs or filaments (Lada & Lada 2003). The spatial distribution of stars in these clusters can be described as a fractal pattern and quantified by a single parameter (e.g. Cartwright & Whitworth 2004; Sánchez & Alfaro 2009). It seems that the original clumpy structure in some clusters tends to be erased with age giving rise to radial density profiles, although clusters as old as ∼100 Myr may still present fractal patterns (Sánchez & Alfaro 2009). However, there exist a number of different possible morphologies and alternative scenarios have been proposed in which structurally simple clusters are built up through hierarchical merging of smaller subclusters (Kuhn et al. 2014, 2015). Thus, a key question is whether the clumpy internal structure observed in some clusters is just the imprint of the parental gas cloud, a signature that tends to disappear over time, or whether new blobs can be generated and/or maintained during the cluster dynamical evolution. A suitable strategy to address this problem is to find clusters having evidence of internal clumpiness and then collect and analyse in detail the spatial and kinematic information available for them. Galactic

open clusters showing signatures of spatial substructure have been previously detected and analysed. Most examples refer to young ($\lesssim$5 Myr) clusters whose structure can be mainly attributed to their original clouds (Lada & Lada 2003; Gregorio-Hetem et al. 2015), for instance, NGC 1333 (Lada, Alves & Lada 1996) and NGC 2264 (Főrész et al. 2006). Intermediate-age (a few times 100 Myr) open clusters with clear evidence of spatial substructures include NGC 2287, NGC 2516 and NGC 2548 (Bergond, Leon & Guibert 2001). Irregular patterns have been also observed in old ($\gtrsim$1 Gyr) clusters like M67 (Davenport & Sandquist 2010) and recently in NGC 6791 (Dalessandro et al. 2015). The irregular overdensities observed in intermediate-age and old clusters are interpreted as associated with real structures stretched by the Galactic potential field (Bergond et al. 2001), but the details of this mechanism can only be fully evaluated through an accurate analysis of the kinematics of cluster members on a large spatial scale to compare core and halo dynamics. The search of patterns or substructures in the velocity phase space requires further improvement both in specific searching tools (e.g. Alfaro & González 2016) and in the precision of the kinematic data. Precise radial velocity measurements have allowed to resolve clumpy structures in four clusters: NGC 2264 (Főrész et al. 2006; Tobin et al. 2015), Orion Nebula Cluster (Főrész et al. 2008), Gamma Velorum (Jeffries et al. 2014) and NGC 2547 (Sacco et al. 2015). There is not, to our knowledge, any reported evidence of grouping or patterns in the proper motion subspace.

From the above mentioned clusters, NGC 2548 is contained in the *Carte du Ciel* – San Fernando (CdC-SF) astrometric catalogue (Vicente et al. 2010). The CdC-SF catalogue presents some advantages over proper motion data currently available for this cluster. It contains precise measurements ($\sim$2 mas yr^{-1} for stars to V $\sim$ 16 and $\sim$1.2 mas yr^{-1} for V $\sim$ 14) which means a deeper extension of *Hipparcos*, in terms of proper motions, up to a magnitude of 14. In this work we use these data to study the properties of NGC 2548, both in spatial coordinates and in proper-motion space. NGC 2548 (M48) is a well-known open cluster with many studies since the second half of 20th century providing extensive knowledge of its main physical properties. It is located in the third Galactic quadrant with coordinates $\alpha = $ 08h 13m 43s and $\delta = -05° 45'$ (Dias et al. 2002). The latest studies generally agree on a distance value in the range 700–780 pc, a very low reddening $E(B - V) = 0$–0.1 and nearly solar metallicity (Wu et al. 2002; Rider et al. 2004; Balaguer-Núñez, Jordi & Galadí-Enríquez 2005; Sharma et al. 2006; Wu et al. 2006; Barnes et al. 2015). The most recent age estimation, based on stellar rotation periods, yielded 450 ± 50 Myr (Barnes et al. 2015) in well agreement with previously determined isochrone ages (Rider et al. 2004; Balaguer-Núñez et al. 2005). This cluster is specially suitable for dynamical evolution studies because of its internal clumpy structure formed by three well differentiated blobs (see fig. 5 in Bergond et al. 2001), but the available kinematic data suffer from one or more of the following drawbacks: (a) small number of data points, (b) limited to relatively bright stars, (c) partial covering of the cluster area and (d) large proper motion uncertainties. By using data from the CdC-SF catalogue, we are able to overcome these issues and to carry out a detailed analysis of the internal structure of NGC 2548. This paper is organized as follows. Section 2 describes the observational data used in this work. Cluster memberships are derived in Section 3 and then used to calculate the spatial and kinematic distribution of stars in Section 4. These results are discussed in Section 5 in the context of the dynamical evolution of star clusters. Finally, the main conclusions are summarized in Section 6.

2 SAMPLE OF STARS

We use the CdC-SF astrometric catalogue (Vicente et al. 2010) which provides precise positions and proper motions for stars up to a magnitude of V $\sim$ 16. The mean positional uncertainty is 0.20 arcsec (0.12 arcsec for well-measured stars) and the proper motion uncertainty is 2.0 mas yr^{-1} (1.2 mas yr^{-1} for well-measured stars). For extracting the data from this catalogue we choose a circle centred on the cluster coordinates given by Dias et al. (2002), $\alpha = $ 123.43 deg and $\delta = -5.75$ deg, that we will assume as the cluster centre in this work. As discussed in Sánchez, Vicente & Alfaro (2010), a proper choice of the sampling radius is crucial to avoid some biases and problems determining memberships and, therefore, the remaining cluster properties. We tried to follow the recipe suggested in Sánchez et al. (2010), based on analysing memberships for several sample radii, but given the irregular space and velocity distributions of stars in this cluster (see next sections) this has not been possible. In any case, the optimal sampling radius nearly coincides with the cluster radius itself (Sánchez et al. 2010); however, it is rather unreliable to estimate this radius from the cluster members available in the literature because, independently of the used method, assigned members tend to spread throughout the area selected by the author. This fact produces discrepancies in the derived radius values. From the projected radial density of stars it is possible to estimate the 'tidal' radius as the point where the radial density becomes roughly constant and merges with the field star density. In this way, tidal radius values ranging from $\sim$8 arcmin (Sharma et al. 2006) to $\sim$43.8 arcmin (Kharchenko et al. 2005) have been reported. We have calculated the surface density of stars (Fig. 1) from which we obtain $R = 45$ arcmin as the optimal sampling radius. With this radius we extract positions and proper motions for the stars in the CdC-SF catalogue in the direction centred at the NGC 2548 coordinates. The total number of stars in our sample is 1655.

From the previous studies of NGC 2548 with photometric data available online (Rider et al. 2004; Balaguer-Núñez et al. 2005;
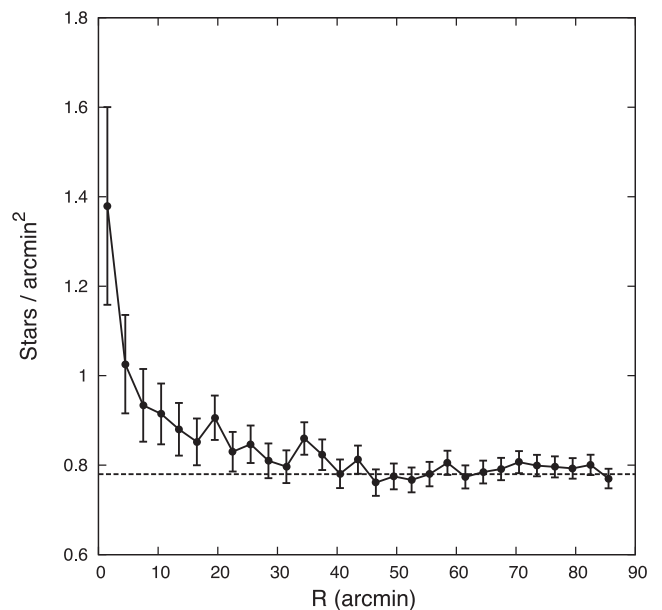

Figure 1. Radial density profile of stars towards NGC 2548. Error bars are from Poisson statistics. Horizontal dashed line indicates the mean value of 0.78 stars arcmin^{-2} calculated from $R = 45$ arcmin, that we consider as optimal sampling radius.
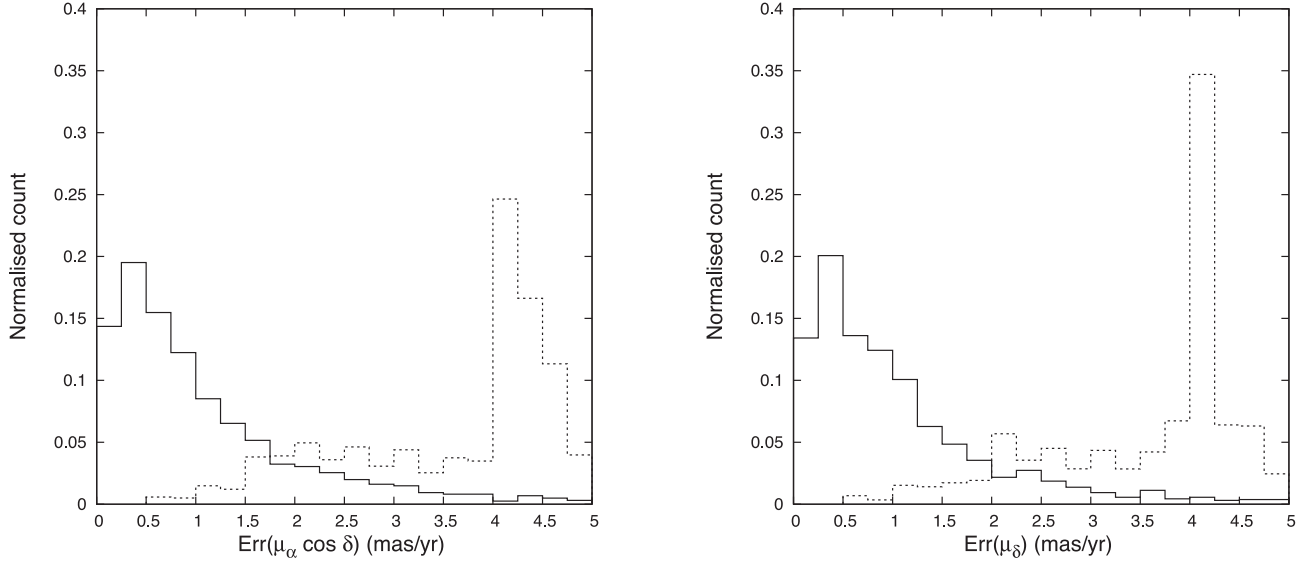
Figure 2. Distribution of proper motion errors in right ascension (left-hand panel) and declination (right-hand panel) for all the stars in our sample. Solid lines correspond to data from the CdC-SF catalogue whereas dashed lines refer to UCAC4.

Wu et al. 2006; Barnes et al. 2015), we note that either the sample of stars is too small for our purposes or the studied area does not fully cover the area we are analysing here. What we have done is to complete our spatial and kinematic information with photometric data from the UCAC4 catalogue (Zacharias et al. 2013), which have photometry for ~113 millions of stars covering the entire sky in the *BgVri* bands supplemented with *JHK* from 2MASS (Skrutskie et al. 2006). Both catalogues were matched by moving CdC-SF positions from 1900 to the UCAC4 mean epoch 2000 and then finding the nearest star in UCAC4 for each star in CdC-SF. Position differences were smaller than 0.2 arcsec (the CdC-SF mean positional uncertainty) for almost all stars. For the cases for which separations were $\gtrsim 0.2$ arcsec we additionally verified that proper motions from CdC-SF and UCAC4 did not differ within their respective uncertainties. Fig. 2 shows the errors in proper motion for our sample of stars compared with the errors extracted from the UCAC4 catalogue. The mean value of our errors is ~1.0 mas yr^{-1} and the median is ~0.7 mas yr^{-1}. The peak of the error distribution lies at $\lesssim 0.5$ mas yr^{-1}, which is much smaller than the ~4 mas yr^{-1} corresponding to UCAC4 (Zacharias et al. 2013). As mentioned before, the main advantage of using the CdC-SF catalogue is the relatively high precision in the proper motion values that will allow us to obtain reliable kinematic memberships and to study with

unprecedented detail the proper motion distribution. Thus, in this work we are using positions and proper motions from the CdC-SF catalogue whereas the photometric values are taken from UCAC4. Table 1 lists positions (Equinox=J2000, Epoch=2000.0), proper motions, photometry and membership probabilities (calculated in next section) for the full sample of stars we have considered in this work.

3 MEMBERSHIP DETERMINATION

The classical method to determine membership probabilities from proper motion data was originally proposed by Vasilevskis, Klemola & Preston (1958) and later revised by Sanders (1971) in the sense of fitting techniques. The method assumes that the global distribution of proper motions can be fitted as the sum of two components, cluster and field, represented by two Gaussian functions. Here we use the improved procedure developed by Cabrera-Caño & Alfaro (1985) which uses a more robust and efficient iterative algorithm for the estimation of the model parameters. Although the method detects and rejects outliers, we have previously removed those stars having too high proper motions (outside the range ±40 mas yr^{-1}) and/or stars with proper motion errors higher than 5 mas yr^{-1} in order to avoid unrealistic fitting solutions. Moreover, to take into

Table 1. List of the 1655 stars towards NGC 2548. This is only a portion for guidance regarding its form and content. The full table is available online.

| UCAC4-ID (col 1)	α (deg) (col 2)	δ (deg) (col 3)	$\mu_\alpha\cos\delta$ (mas yr^{-1}) (col 4 ± 5)	μ_δ (mas yr^{-1}) (col 6 ± 7)	Prob. (col 8)	B (UCAC4) (col 9 ± 10)	V (UCAC4) (col 11 ± 12)
421 − 044734	122.6813	−5.8258	− 3.44 ± 0.17	+2.07 ± 0.24	0.92	13.99 ± 0.02	13.56 ± 0.01
422 − 043693	122.6840	−5.6603	− 14.10 ± 10.02	+15.65 ± 1.52	0.00	−	−
421 − 044741	122.6892	−5.8644	+0.65 ± 0.40	− 1.98 ± 0.24	0.84	13.83 ± 0.01	13.31 ± 0.02
422 − 043697	122.6908	−5.6704	− 4.02 ± 1.24	+0.98 ± 1.80	0.89	14.87 ± 0.02	14.19 ± 0.01
422 − 043698	122.6916	−5.6399	− 6.96 ± 1.52	+6.29 ± 1.71	0.79	14.99 ± 0.03	14.40 ± 0.03
421 − 044744	122.6929	−5.8273	− 5.01 ± 0.37	− 2.22 ± 0.35	0.55	10.59 ± 0.08	9.75 ± 0.10
421 − 044745	122.6931	−5.8574	− 3.89 ± 0.32	+4.65 ± 0.32	0.93	13.28 ± 0.01	12.28 ± 0.00
423 − 045526	122.6977	−5.5697	− 1.09 ± 0.40	+5.67 ± 1.24	0.93	13.59 ± 0.04	12.56 ± 0.01
421 − 044751	122.6983	−5.8903	+1.95 ± 1.14	− 3.54 ± 1.71	0.68	14.75 ± 0.03	14.03 ± 0.03
422 − 043700	122.6997	−5.7492	− 4.97 ± 0.58	− 2.97 ± 0.32	0.43	14.14 ± 0.03	13.59 ± 0.02
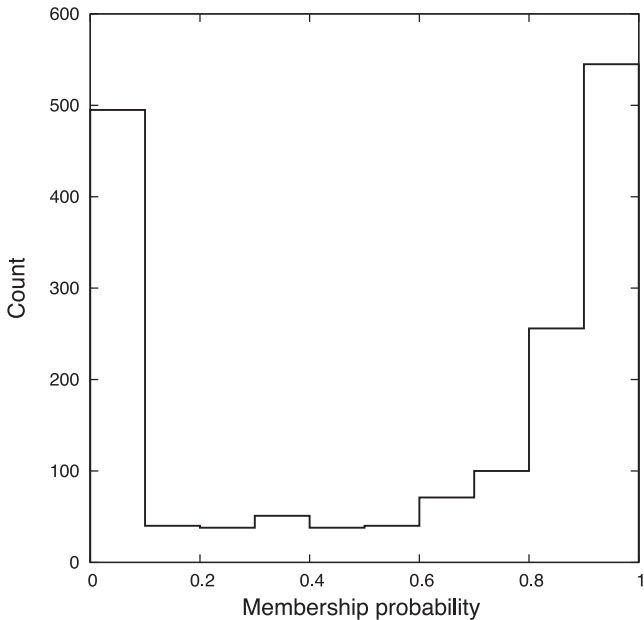
Figure 3. Histogram of cluster membership probabilities for stars in NGC 2548.

Table 2. Kinematic parameters for NGC 2548.

	N/N_t	ρ	$\mu_\alpha \cos\delta$ (mas yr^{-1})	μ_δ (mas yr^{-1})	$\sigma_{\mu_\alpha \cos\delta}$ (mas yr^{-1})	σ_{μ_δ} (mas yr^{-1})
NGC 2548	0.61	−0.26	−1.55	+3.16	+3.09	+3.31
Field	0.39	−0.11	−4.04	−0.05	+9.61	+10.28

account the possibility of asymmetries in the velocity space, we do not use a circular Gaussian distribution for the cluster but a Gaussian function with dispersions that can be different in right ascension and declination.
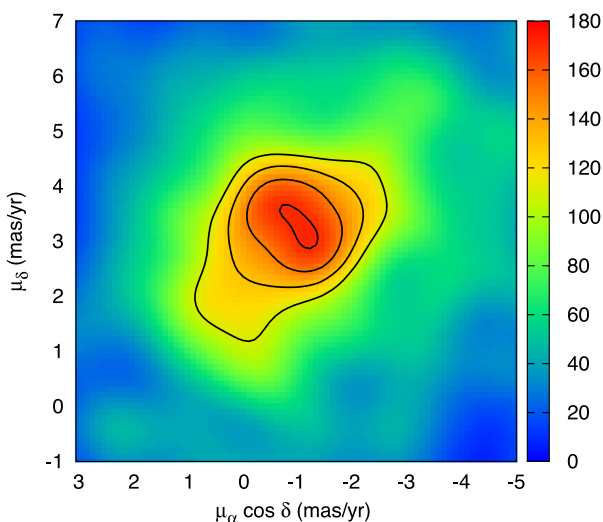
The application of the algorithm to our data yielded all star membership probabilities p as well as the final kinematic parameters for cluster and field. Fig. 3 is the histogram of membership probabilities where we can see that cluster and field stars are clearly separated. There is a total of 1012 members ($p > 0.5$). The obtained kinematic parameters for both cluster and field, including the fraction of stars (N/N_t), the correlation coefficient (ρ), the proper motion in right ascension and declination ($\mu_\alpha \cos\delta$ and μ_δ) and their corresponding dispersions ($\sigma_{\mu_\alpha \cos\delta}$ and σ_{μ_δ}), are summarized in Table 2. We can see that cluster and field are two populations that have been clearly differentiated by the algorithm.

4 SPATIAL AND KINEMATIC DISTRIBUTION OF STARS

In order to calculate the spatial and kinematic density of member stars in NGC 2548, we perform a direct estimation using Kernel functions of the form

$$f(x, y) = \frac{1}{Nh^2} \sum_{i=1}^{N} K\left(\frac{x - x_i}{h}, \frac{y - y_i}{h}\right) \qquad (1)$$

being x, y the spatial or kinematic variables and where a Gaussian Kernel function K is summed over the sample of N members. The final density estimation depends considerably on the value of the smoothing parameter h. To avoid either very large h values that over-smooth the distribution or small values that produce noisy solution, we always use the h value such that the likelihood is maximum (see details in Silverman 1986; Cabrera-Caño & Alfaro 1990). For the spatial coordinates the optimal smoothing parameter was $h = 3.6$ arcmin whereas for the proper motion space was $h = 0.5$ mas yr^{-1}.

The resulting density maps are shown in Fig. 4. The distribution of proper motions (left-hand panel in Fig. 4) is far from being the circular distribution expected for typical open clusters. The global shape of the proper motion distribution is rather elongated, but interestingly the central part of the distribution is elongated along the direction perpendicular to the global shape. On the other hand, the spatial star distribution (right-hand panel in Fig. 4) is quite complex.
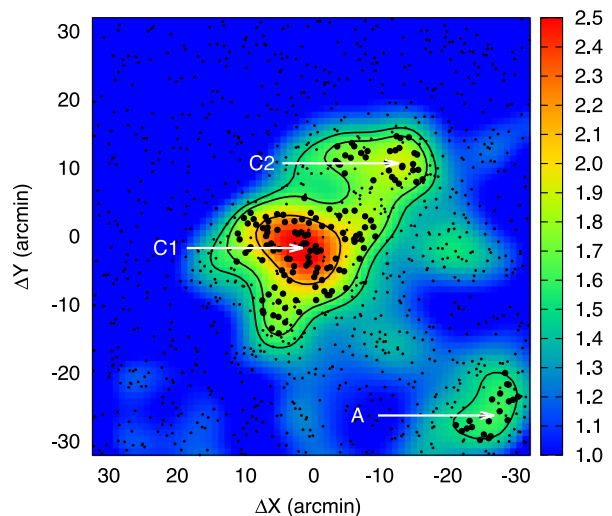

Figure 4. Left-hand panel: star density in the proper motion space for the members of NGC 2548. Equally spaced isocontours from 110 to 170 stars per (mas yr^{-1})^2 are shown. Right-hand panel: spatial density of member stars in NGC 2548 (positions are relative to the cluster's centre). The colour scale runs from 1.0 a 2.5 stars arcmin^{-2} being the average of the field ∼0.8 stars arcmin^{-2}. Isocontours are shown for 1.50, 1.65 and 2.10 stars arcmin^{-2} corresponding to percentiles 90, 95 and 99 per cent, respectively. Arrows indicate each one of the three identified maxima that we associate with the three cores denoted by C1, C2 and A. Small black dots are cluster members and bigger black points correspond to the stars selected as belonging to these cores (see details in the text).
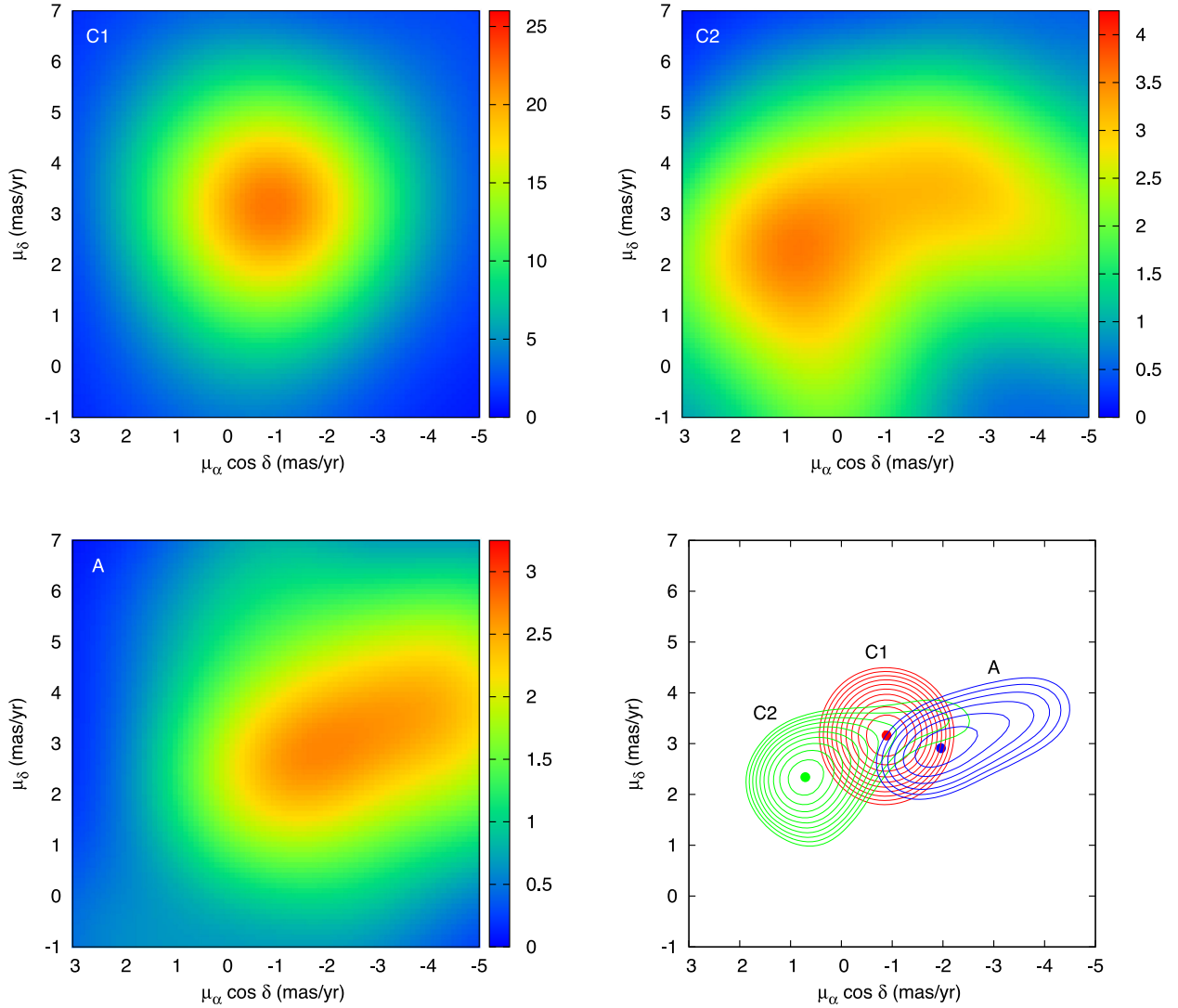
Figure 5. Star density in the proper motion space for the stars belonging to cores C1 (upper left panel), C2 (upper right) and A (lower left). Equally spaced isocontours above the 95th percentile are shown together in the lower right panel.

We can see an irregular main structure, consisting of a relatively dense central core (marked as C1) and a less dense secondary core (C2) clearly detached from the main core. Additionally, there is a slight overdensity in SW direction (marked as A) well separated from the two central cores. These features (C1, C2 and A), that were already described by Bergond et al. (2001), stand out clearly over the mean field star density, which is ∼0.8 stars arcmin^{-2}. The main core (C1) peaks with 2.6 stars arcmin^{-2} at $(\Delta X, \Delta Y) = (+1.2, -1.7)$ arcmin relative to the assumed centre of NGC 2548 (taken from Dias et al. 2002), whereas C2 shows a peak of 1.9 stars arcmin^{-2} at $(\Delta X, \Delta Y) = (-12.8, +10.7)$ arcmin. The maximum value for A is 1.6 stars arcmin^{-2} and is located at $(\Delta X, \Delta Y) = (-26.8, -26.2)$ arcmin.

In order to describe in more detail their kinematic properties, we have selected the stars belonging to each of the observed substructures. For the selection we have taken into account the isocontours shown in the right-hand panel of Fig. 4 that correspond to the percentiles 90, 95 and 99 per cent of the surface density values. Then we select approximately the stars inside these isocontours and associate them to each core based on their proximity to the density peaks. For the two main cores (C1 and C2) we use the 95th per-

centile as threshold whereas for A we use the 90th. The resulting selection is indicated in Fig. 4 as black points. Once selected, we recalculate the kinematic density distribution for each core, following the same previous procedure. The result is shown in Fig. 5. We note that each substructure (core) seen in the spatial distribution of stars have a well differentiated counterpart in the proper motion space. Proper motions of core C1 follow a somewhat regular, circular distribution with the maximum located at $(\mu_\alpha \cos \delta, \mu_\delta) = (-0.89, +3.16)$ mas yr^{-1}. Cores C2 and A exhibit more irregular distributions with less pronounced maxima at $(\mu_\alpha \cos \delta, \mu_\delta) = (+0.71, +2.34)$ mas yr^{-1} and $(\mu_\alpha \cos \delta, \mu_\delta) = (-1.96, +2.91)$ mas yr^{-1}, respectively. The C1–C2 and C1–A centroid separations in the vector-point diagram are ∼1.8 and ∼1.1 mas yr^{-1}, respectively, above the typical error for our proper motion values.

It is the first time, to our knowledge, that a clumpy structure in the proper motion space is detected in an open cluster, where each core centroid can be unequivocally associated with a corresponding spatial blob. In general terms, the proper motions of these three substructures explain the observed kinematic distribution shown in left-hand panel of Fig. 4: the combination of the proper motions of C1 and C2 produces the global ellipsoidal shape whereas the

Table 3. Derived properties for the three cores observed in NGC 2548.

Core	N	ΔX (arcmin)	ΔY (arcmin)	$\mu_\alpha \cos \delta$ (mas yr^{-1})	μ_δ (mas yr^{-1})
C1	106	$+1.2$	-1.7	-0.89	$+3.16$
C2	34	-12.8	$+10.7$	$+0.71$	$+2.34$
A	21	-26.8	-26.2	-1.96	$+2.91$

combination with core A generates the perpendicular elongation in the central part of the distribution. Clump C1 is nearly spherical in both position and proper motion space whereas C2 can be considered as a small perturbation on the bulk of the cluster. Clump A, on the other hand, is a weak overdensity whose precise nature is uncertain (see discussion later). Table 3 summarizes the derived properties for each core observed in NGC 2548, including the number of stars N, their positions relative to the assumed cluster centre and their representative proper motions. Both positions and proper motions refer to the maxima of their density distributions. We have verified that the detection and shapes of these substructures are not very sensitive to the exact value of the chosen sampling radius and to the exact number of assigned members. Peak densities observed in right-hand panel of Fig. 4 are 2 to 3 times over the background density. Interestingly, membership probability values for stars belonging to the clumps are, in general, relatively high (see Table 1) so that if we set, for instance, a more restrictive membership threshold the total number of cluster members decreases but clump members decrease in a smaller proportion, in such way that the observed density peaks remain unchanged or even increase relative to the cluster background.

4.1 Cluster photometry

Fig. 6 shows the V versus $B - V$ diagram for all member stars in NGC 2548. Main sequence is clearly visible and is fairly
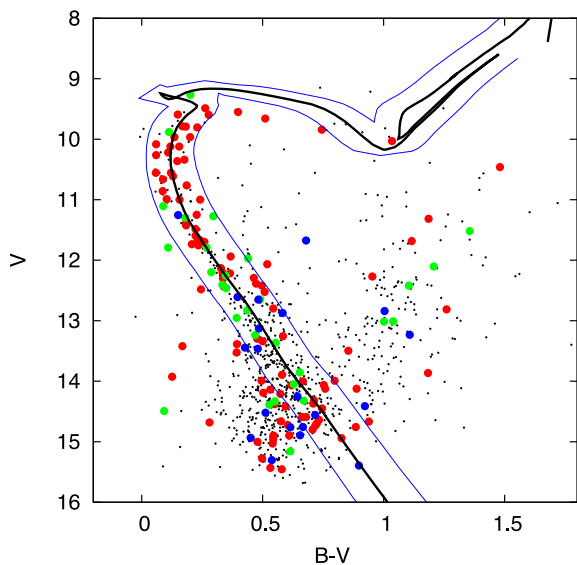

Figure 6. Colour–magnitude diagram for all members of NGC 2548. Red, green and blue circles mark stars belonging to cores C1, C2 and A, respectively. As a reference, we have also plotted (solid black line) the Padova isochrone (Bressan et al. 2012) of age 500 Myr, $E(B - V) = 0.1$, solar metallicity, and distance 780 pc. Blue lines define a band around this isochrone to allow for an uncertainty of three times the mean error in magnitude (0.020) and colour (0.032) and to consider the effects of binarity.
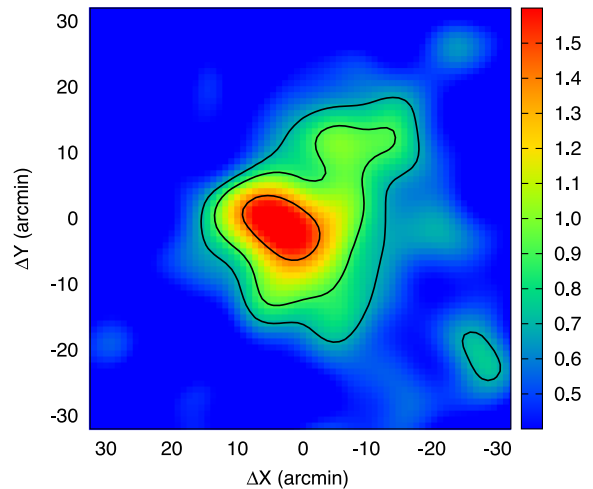
Figure 7. Spatial density for stars that are kinematic and also photometric members of the cluster (see the text). Colour scale runs from 0.4 to 1.6 stars arcmin^{-2} and isocontours are shown for percentiles 90, 95 and 99 per cent.

well fitted with an isochrone corresponding to a slightly reddened $[E(B - V) = 0.1]$ cluster of age of 500 Myr located at 780 pc. Most stars associated with cores C1, C2 and A (coloured circles in Fig. 6) lie on the main sequence. We see that stars belonging to the double core C1–C2 (red and green circles) mostly follow the isochrone upper-tail, while stars in core A appear fainter and spread out over the lower-tail of the $(B, B - V)$ diagram. The minimum magnitude for core A is $V \sim 11.3$ with a median of ~ 14.3, which is two magnitudes higher than the C1–C2 median magnitude (~ 12.4). Given that NGC 2548 is a practically non-extincted cluster, this means that core A stars are on average less luminous than C1–C2 stars.

Stars plotted in Fig. 6 are all the kinematically selected members of NGC 2548, although we see that a few stars have magnitude and colour values such that they are not cluster members from a photometric point of view. In this work we have left cluster memberships unaltered because the issue of kinematic versus photometric (or combined kinematic-photometric) cluster memberships, their reliabilities and possible effects on the derived cluster properties is out of the scope of this paper. However, in order to evaluate the robustness of our results we performed some additional tests. We defined a region around the considered isochrone in the $B-V$ colour–magnitude diagram (delimited by blue lines in Fig. 6), then we selected as kinematic *and* photometric members those stars lying inside this area and we recalculated the spatial density of stars as before. The result is shown in Fig. 7 and Table 4 summarizes some core properties for the cases of only kinematically selected members and also photometrically selected members in the $B-V$

Table 4. Comparison of core properties for kinematically selected and kinematically plus photometrically selected cluster members (density unit is stars arcmin^{-2}).

Property	Kinematic members	Photometric members
Cluster members	1012	438
Mean cluster density	0.8	0.3
Core stars (C1, C2, A)	106, 34, 21	68, 18, 9
Percentile (Q99, Q95, Q90)	2.1, 1.7, 1.5	1.3, 0.9, 0.7
Peak density (C1, C2, A)	2.6, 1.9, 1.6	1.8, 1.0, 0.8

diagram.[1] The number of cluster members and therefore the mean star density decrease but, as it happened when we applied a more restrictive kinematic membership selection threshold, core members decrease in a smaller proportion and their density peaks increase relative to the background. As before, core A is seen above the 90th percentile but as a weak overdensity with few members.

5 DISCUSSION

Our main result is the finding that each substructure observed in the spatial distribution of stars in NGC 2548 has its well differentiated counterpart in the proper motion space, which provides the first *kinematic* evidence of cluster disruption occurring in this stellar system. As far as we know, this is the first detection of a clumpy structure in the proper motion space in any star cluster. As discussed by Bergond et al. (2001), the spatial clumpy structure observed in NGC 2548 is likely a consequence of its interaction with the Galactic gravitational field. As clusters move on their orbits through the Milky Way, they will pass several times through the Galactic disc and they may become morphologically disturbed or even destroyed due to the Galactic tidal forces (Terlevich 1987). Successive passes through the Galactic plane can speed up the destruction of clusters, although the ease with which they can be destroyed depends on variables such as the initial mass function or the initial virial state, and the expected disruption time-scale varies from less than ~100 Myr up to the order of ~1 Gyr (de La Fuente Marcos 1997). Other possible disruption mechanisms, such as close encounters with giant molecular clouds, do not seem to be as effective as Galactic tides in disrupting open cluster (Terlevich 1987; Gieles et al. 2006).

The relative spatial configuration of the three internal cores in NGC 2548 suggests a predominant interaction with Galactic forces. Fig. 8 shows the spatial distribution of the cores, also indicating their proper motions relative to the cluster centroid and the directions perpendicular and parallel to the Galactic plane. The stretching of C1–C2 is nearly parallel to the Galactic plane, which is consistent with the flattening in the same direction predicted in numerical simulations (Terlevich 1987). On the other hand, clump A is located relatively far from the main cores at ~8.5 pc in the direction of the Galactic plane. This was interpreted by Bergond et al. (2001) as A being a remnant of the last disc-shocking of NGC 2548. Note that A's proper motion relative to the cluster centroid (black arrows in Fig. 8) goes towards the Galactic plane and away from the rest of the cluster.

Nevertheless, it must be pointed out that it is not possible to be sure about the real nature of clump A. Given that it is a weak overdensity with few members and it seems to be detached from the main cluster (cores C1–C2), a random concentration of field stars is also a plausible explanation for the origin of this clump. However, we should note that we are not estimating spatial overdensities from the full star sample without any rigorous membership analysis (as in Bergond et al. 2001), but after a reliable kinematic membership assignment. The fact that clump A is inside our estimated cluster radius together with the fact that its presence is robust against the kinematic pruning of the data point towards a real star clump moving away from the central part. There is still the alternative possibility that clump A is a small spatial overdensity of stars but lying at
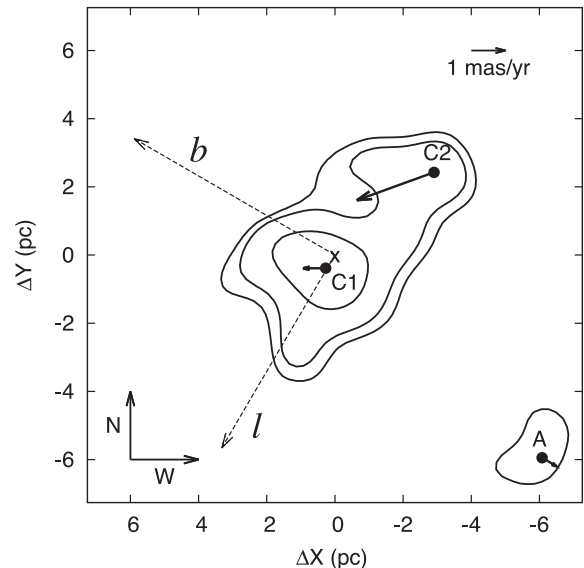

Figure 8. Simplified version of Fig. 4 (right-hand panel) showing the higher density isocontours and positions of cores C1, C2 and A. Solid arrows represent the proper motions of the cores relative to the global proper motion of the cluster derived in Section 3. Reference arrow in upper right corner has a length of 1 mas yr^{-1}. Dashed arrows indicate axes parallel (*l*) and perpendicular (*b*) to the Galactic plane, respectively.

some distance behind NGC 2548. This alternative is supported by the, on average, fainter magnitudes of their stars but, in this case, the kinematic similarities have to be interpreted as happening by chance. If we take as true that A is a clump that has been separated from the original cluster by tidal forces, then the kinematic solutions are consistent because A goes away from the rest of the cluster due to its last pass through the Galactic disc. The challenge in this case is to understand why the core A is on average less luminous than C1–C2. There must have been some mass-segregation episode either associated with the dynamical disruption itself or with a primordial mass-segregated pattern.

There are many open clusters showing elongations or other shape distortions (Chen, Chen & Shu 2004). For a very young open cluster, its morphological structure is likely determined by the initial conditions in the parental cloud (Sánchez & Alfaro 2009); but for dynamically evolved clusters, external tidal perturbations would become increasingly important. In fact, cluster properties such as size or flattening seem to correlate with distances to the Galactic Centre and plane probably because these variables define the degree of tidal stress (Chen et al. 2004; Bonatto & Bica 2010). It would be necessary to extend this type of analysis to large samples of disrupting star cluster candidates (as, for instance, those in Bica et al. 2001). *Gaia* data will be particularly useful for this because it will measure very precise proper motion values even for low-mass members in open clusters. In this work, we were able to detect kinematic substructures because of our relatively precise proper motions (mean error ~1.0 mas yr^{-1}, four times better than UCAC4), but *Gaia* expected mean errors are ~0.08 mas yr^{-1} (about 10 times smaller than ours) or even ~0.02 mas yr^{-1} for bright stars with $G < 15$ (Luri et al. 2014). Moreover, *Gaia* will also provide radial velocities that make it possible to derive reliable three-dimensional space velocities. This will allow to perform detailed statistical studies to better understand the cluster destruction processes and how they depend on cluster environmental properties such as Galactic location and orbit.

---

[1] We did several tests considering different photometric bands and the results remain qualitatively similar. Here we show the $B-V$ case as an example, a rigorous photometric analysis would involve several photometric bands simultaneously.

6 CONCLUSIONS

We have used precise astrometric data from the CdC-SF catalogue to analyse the spatial and kinematic structure of the open cluster NGC 2548. From the spatial distribution of reliable cluster members we confirm its previously reported fragmented structure consisting of three separated cores (denoted as C1, C2 and A) but, for the first time, we also distinguish the corresponding blobs in the proper motion space. The two main cores C1 and C2 are aligned nearly parallel to the Galactic plane whereas the fainter and less dense core A moves towards the plane and appears to be detaching itself from the rest of the cluster. We present the derived core properties in Table 3. This clumpy spatial and kinematical structure observed in NGC 2548 could be consequence of the Galactic gravitational field, in particular due to its last crossing through the Galactic plane.

REFERENCES

Alfaro E. J., González M., 2016, MNRAS, 456, 2900
Balaguer-Núñez L., Jordi C., Galadí-Enríquez D., 2005, A&A, 437, 457
Barnes S. A., Weingrill J., Granzer T., Spada F., Strassmeier K. G., 2015, A&A, 583, A73
Bergond G., Leon S., Guibert J., 2001, A&A, 377, 462
Bica E., Santiago B. X., Dutra C. M., Dottori H., de Oliveira M. R., Pavani D., 2001, A&A, 366, 827
Bonatto C., Bica E., 2010, A&A, 521, A74
Bressan A., Marigo P., Girardi L., Salasnich B., Dal Cero C., Rubele S., Nanni A., 2012, MNRAS, 427, 127
Cabrera-Caño J., Alfaro E. J., 1985, A&A, 150, 298
Cabrera-Caño J., Alfaro E. J., 1990, A&A, 235, 94
Cartwright A., Whitworth A. P., 2004, MNRAS, 348, 589
Chen W. P., Chen C. W., Shu C. G., 2004, AJ, 128, 2306
Dalessandro E., Miocchi P., Carraro G., Jílková L., Moitinho A., 2015, MNRAS, 449, 1811
Davenport J. R. A., Sandquist E. L., 2010, ApJ, 711, 559
de La Fuente Marcos R., 1997, A&A, 322, 764
Dias W. S., Alessi B. S., Moitinho A., Lépine J. R. D., 2002, A&A, 389, 871
Elmegreen B. G., 2006, ApJ, 648, 572
Elmegreen B. G., Efremov Y. N., 1996, ApJ, 466, 802
Elmegreen B. G., Hunter D. A., 2010, ApJ, 712, 604
Fall S. M., Chandar R., Whitmore B. C., 2005, ApJ, 631, L133
Fűrész G. et al., 2006, ApJ, 648, 1090
Fűrész G., Hartmann L. W., Megeath S. T., Szentgyorgyi A. H., Hamden E. T., 2008, ApJ, 676, 1109
Leenaarts, J.Gieles M., Portegies Zwart S. F., Baumgardt H., Athanassoula E., Lamers H. J. G. L. M., Sipior M., 2006, MNRAS, 371, 793
Gregorio-Hetem J., Hetem A., Santos-Silva T., Fernandes B., 2015, MNRAS, 448, 2504
Jeffries R. D. et al., 2014, A&A, 563, A94
Kharchenko N. V., Piskunov A. E., Röser S., Schilbach E., Scholz R.-D., 2005, A&A, 438, 1163
Kruijssen J. M. D., Pelupessy F. I., Lamers H. J. G. L. M., Portegies Zwart S. F., Icke V., 2011, MNRAS, 414, 1339
Kuhn M. A. et al., 2014, ApJ, 787, 107
Kuhn M. A. et al., 2015, ApJ, 812, 131
Lada C. J., 2010, Phil. Trans. R. Soc. A, 368, 713
Lada C. J., Lada E. A., 2003, ARA&A, 41, 57
Lada C. J., Alves J., Lada E. A., 1996, AJ, 111, 1964
Luri X. et al., 2014, A&A, 566, A119
Oort J. H., 1958, Ric. Astron., 5, 415
Parker R. J., 2014, in Stamatellos D., Goodwin S., Ward-Thompson D., eds, Astrophys. Space Sci. Proc. Vol. 36, The Labyrinth of Star Formation. Springer International Publishing, Switzerland, p. 431
Parker R. J., Wright N. J., Goodwin S. P., Meyer M. R., 2014, MNRAS, 438, 620
Piskunov A. E., Kharchenko N. V., Schilbach E., Rööser S., Scholz R.-D., Zinnecker H., 2008, A&A, 487, 557
Rider C. J., Tucker D. L., Smith J. A., Stoughton C., Allam S. S., Neilsen E. H., 2004, AJ, 127, 2210
Sacco G. G. et al., 2015, A&A, 574, L7
Sánchez N., Alfaro E. J., 2009, ApJ, 696, 2086
Sánchez N., Vicente B., Alfaro E. J., 2010, A&A, 510, A78
Sanders W. L., 1971, A&A, 14, 226
Sharma S., Pandey A. K., Ogura K., Mito H., Tarusawa K., Sagar R., 2006, AJ, 132, 1669
Silverman B. W., 1986, Monographs on Statistics and Applied Probability, Chapman and Hall, London
Skrutskie M. F. et al., 2006, AJ, 131, 1163
Terlevich E., 1987, MNRAS, 224, 193
Tobin J. J., Hartmann L., Fűrész G., Hsu W.-H., Mateo M., 2015, AJ, 149, 119
Tutukov A. V., 1978, A&A, 70, 57
Vasilevskis S., Klemola A., Preston G., 1958, AJ, 63, 387
Vicente B., Abad C., Garzón F., Girard T. M., 2010, A&A, 509, A62
Wielen R., 1971, A&A, 13, 309
Wu Z. Y., Tian K. P., Balaguer-Núñez L., Jordi C., Zhao J. L., Guibert J., 2002, A&A, 381, 464
Wu Z.-Y., Zhou X., Ma J., Jiang Z.-J., Chen J.-S., 2006, PASP, 118, 1104
Zacharias N., Finch C. T., Girard T. M., Henden A., Bartlett J., Monet D., Zacharias M., 2013, AJ, 145, 44

SUPPORTING INFORMATION

Additional Supporting Information may be found in the online version of this article:

Table 1. List of the 1655 stars towards NGC 2548.
(http://www.mnras.oxfordjournals.org/lookup/suppl/doi:10.1093/mnras/stw1487/-/DC1).

Please note: Oxford University Press is not responsible for the content or functionality of any supporting materials supplied by the authors. Any queries (other than missing material) should be directed to the corresponding author for the article.

This paper has been typeset from a TeX/LaTeX file prepared by the author.